

Development and Power Calculation of a Grinding Wheel Design for Ultra-High-Speed Grinding

Denis Rechenko^{1,*}, Renat Kamenov¹

¹Omsk State Technical University, RU-644050, Omsk, Russia

Abstract. Increasing the structural reliability at ultra-high-speed grinding is an important problem because it defines safety of metalworking. The purpose of work is to achieve the cutting speed up to 400-500 m/s by developing a new design of the grinding wheel with the possibility of using different grinding materials. Grinding wheel design for ultra-high-speed grinding was developed based on calculations carried out using the tear design method, which allows determining the maximum possible circumferential speed, and finite element method used to determine the equivalent stresses, plastic deformations, circumferential and radial movements. The possibility of development of a grinding wheel design for ultra-high-speed grinding has been tested experimentally. The developed designs of grinding wheels show may possibly be used on super high-speed technological equipment for processing of parts made of hard-to-machine materials. Calculations and comprehensive experimental tests of the design of grinding wheels for ultra-high-speed grinding carried out in this work allow determining the serviceability and the maximum possible cutting speed and provide useful information for the further development of grinding tools.

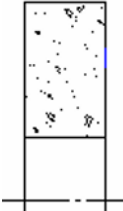

1 Introduction

An analysis of the existing designs of grinding wheels for high-speed grinding shows that the maximum circumferential machining speed of up to 160 m/s can be achieved (Table 1). Standard grinding wheels for high-speed grinding have a strength that allows processing at speeds up to 60-160 m/s [1-17]. After refining the existing designs, it is possible to reach cutting speeds of about 250 m/s in laboratory conditions without any possibility of further industrial applications of the refined design. In the case, when the cutting speed limit is exceeded, the individual components are torn off or the grinding wheel housing is torn apart. There exist the following criteria for the grinding wheel design:

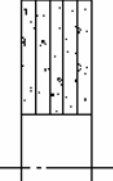
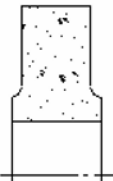
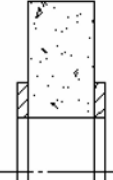
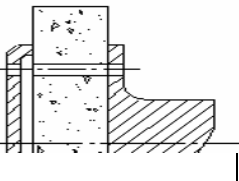
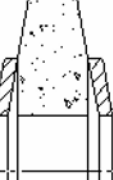
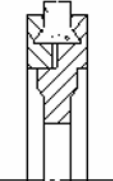
- the grinding wheel can run at the highest possible cutting speed without risk of rupture;
- the ability to use different grinding materials;
- simplicity of design with a minimum number of stress concentrators;
- reliability of the clamping design of grinding segment.

Table 1. Grinding wheel designs.

No	Sketch	Strength	Description of how to increase the strength of a grinding wheel structure
----	--------	----------	---

1		+	Strengthening of the non-working central part of the circle due to the application of fine-grained mixtures forming a dense, strong composition with binder or impregnation of the central part of the circle on the ceramic binder with strong thermoplastic compositions. Working speed - up to 60 m/s.
2		++	Reinforcement of the central part of the circles by pressing in a bushing made of particularly strong materials. Working speed up to 80 m/s.

* Corresponding author: rechenko-denis@mail.ru

3		++	Strengthens circles on the bakelite bond by installing GRP mesh gaskets inside the circle. Working speed - up to 100 m/s.
4		++	Manufacture of circles of variable cross-section with a thickening of the central part, smoothly descending to the working part. Working speed - up to 100 m/s.
5		+++	Hardening due to metal discs glued to the ends of the grinding wheel. Working speed - up to 120 m/s.
6		++++	Sharpening by using a one-piece grinding wheel design with small holes to allow attachment to the plate. Working speed - up to 120 m/s.
7		++++	Reinforcing by using special spring flanges. Working speed - up to 120 m/s.
8		+++++	Peening by the use of prefabricated circular structures consisting of segments attached to the plate. Working speed - up to 160 m/s.

Creating a new design that allows for safe grinding at the highest possible circumferential speed is a complex task that requires a careful consideration of the strength, maximum possible operating speeds, the system of attachment of the grinding elements and fixing the body in the spindle shaft.

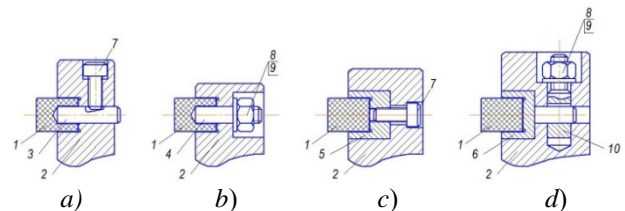
Some designs of grinding wheels include the use of metal bandages, shroud, etc., which significantly reduces the possibility of their rupture. The analysis of the existing designs has been shown that a grinding wheel for ultra-high-speed processing needs an all-metal case with the smallest number of parts and that the safety margin factor should be 1.4 (GOST R 52857.1-2007).

2 Problem statement

Cutting speeds of up to 400-500 m/s can be achieved by designing a new grinding wheel design with the possibility of using different grinding materials. Grinding wheel design for ultra-high-speed grinding was calculated using the tear design method, which allows to determine the maximum possible circumferential speed and finite element method to determine the equivalent stresses, plastic deformations, circumferential and radial movements in the process.

3 Analysis and development of bindings of grinding segment

Development of replaceable grinding segments, namely the circuit and the mechanism of their fixation is an important task, because the performance of the entire process unit depends on it. Different grinding segment characteristics can only be implemented with a one-piece grinding wheel or using with mounting sockets or replacement segments. Studies of aerodynamic work have shown that the most appropriate use of cylindrical grinding segments. From possible schemes of fastening of grinding segments, the author offers and considers the most technological and having a simple design (Fig. 1) [2-7].



1 - grinding head; 2 - body of grinding wheel; 3 - oblique groove pin; 4 - threaded pin; 5 - beaker; 6 - beaker on pin; 7 - fastening bolt; 8 - fastening nut; 9 - washer; 10 - trunnion block

Fig. 1. Fastening structures for replacement grinding segments: a) fastening with a radial bolt; b) fastening with an axial nut; c) fastening with an axial bolt; d) fastening with a radial nut.

The presented designs of fastening of grinding segments provide reliable fastening, thus fastening with a radial bolt (Fig. 1, a) provides simplicity of realization of this design on the basis of standard grinding heads with a pin. The use of the attachment structure with an axial nut (Fig. 1, b) is quite dangerous, as the attachment force also works on detaching the diamond head from the pin. The use of axial bolt fixing (Fig. 1.c) seems to be the most rational, due to the simplicity of its construction and the clamping force being provided exclusively on the bucket in which the grinding segment is located. The design of the attachment with a radial nut (Fig. 1.d) is reliable, but complex in execution and operation.

The results of strength calculations of various abrasive and binder materials are shown in Figure 2, the shear stress dependence on the grinding wheel circumferential speed is presented.

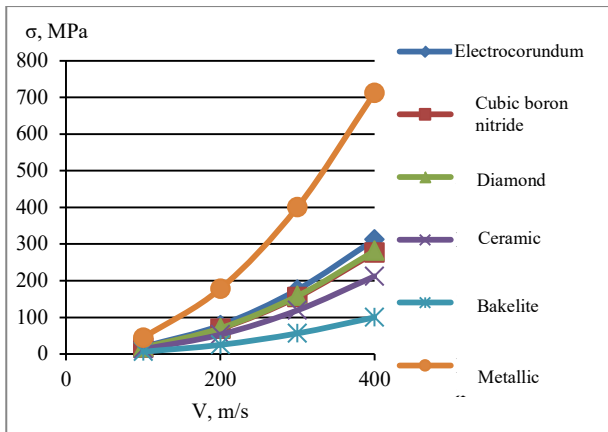


Fig. 2. Cutting voltage dependence on grinding wheel circumferential speed.

It can be seen from the dependence that the bakelite ligament has shear stresses at a speed of 400 m/s about 100 MPa. Standard grinding inserts have a strength limit of about 30–40 MPa, so it is necessary to develop grinding inserts on the bakelite binder, providing the ability to work at speeds up to 400 m/s, while ensuring the appropriate shear strength.

According to the conducted tests, the bending strength limit for the given developed formulations is 120.2...153.8 MPa, which provides the coefficient of safety margin in the range of 1.2–1.5.

The number of grinding segments is determined by the heat dissipation condition during grinding and the effective power condition. When calculating the different number of heads involved in grinding, the working area must be determined. The working surface area of the diamond heads is 4 pcs., is 8% – $S_{heads} = 1257 \text{ mm}^2$ and $S_{work} = 15708 \text{ mm}^2$. Accordingly, at 16 pcs. – $S_{work} = 62832 \text{ mm}^2$.

4 Determining the maximum permissible grinding wheel speed for high-speed machining

Grinding wheel calculation comes down to determining the maximum permissible cutting speed at which a grinding wheel is capable of machining. The maximum circumferential speed of the grinding wheel is influenced by the body material, dimensions and shape. The calculation is carried out for three proposed seating options: nozzle, striking face and end face (Fig. 3), based on the allowable tension on the tension of the material of the body of the circle [8–15].

Grinding wheels for rupture are calculated according to the allowable stress and the stress arising from centrifugal forces from the condition:

$$\sigma \leq [\sigma], \quad (1)$$

where σ – tensile stress arising during operation due to centrifugal forces, MPa; $[\sigma]$ – permissible tensile stress, MPa.

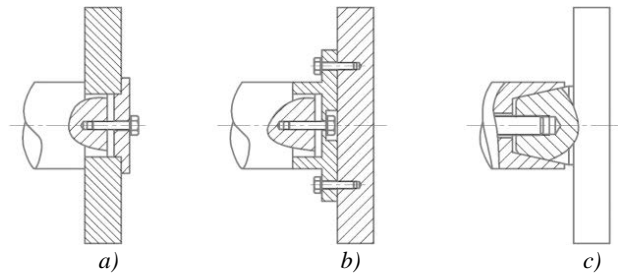


Fig. 3. Fitting options for a nozzle ultra-fast grinding wheel with heel: a) nozzle mount; b) striking mount; c) end mount.

The calculation of tensile stresses is based on formulas:

$$\text{– for a disk } \sigma = \frac{\rho \cdot V_r^2}{2}; \quad (2)$$

$$\text{– for a ring } \sigma = \frac{R \cdot \rho \cdot V_r^2}{R-r}, \quad (3)$$

where ρ – grinding wheel body material density, kg/m^3 ; V_r – linear grinding wheel speed at the calculated radius, m/s; R – calculated grinding wheel radius, m; r – landing radius, m.

Based on the expressions (1, 2 and 3), the maximum allowed circumferential speed is calculated by the formulas:

$$\text{– for a disk } V_r = \sqrt{\frac{2 \cdot [\sigma]}{\rho}};$$

$$\text{– for a ring } V_r = \sqrt{\frac{(R-r) \cdot [\sigma]}{\rho \cdot R}}.$$

Figure 4 and Table 2 show the results of the calculations for different materials. Overall dimensions $R = 125 \text{ mm}$; $r = 38 \text{ mm}$.

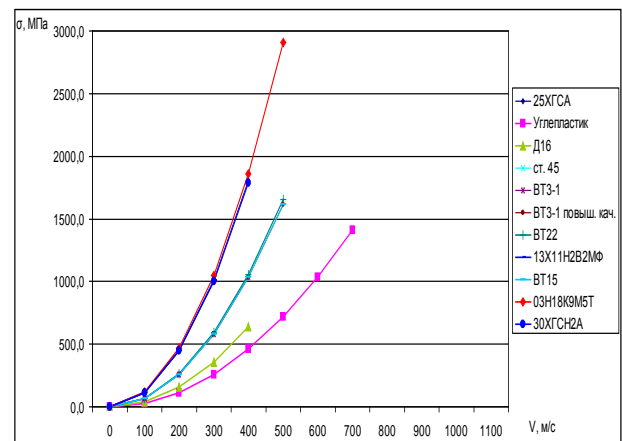


Fig. 4. Dependence of tensile stress on the circumferential speed of the grinding wheel in different materials.

Application of 30KhGSN2A or VT3-1 of the raised quality as the case of a grinding wheel allows to receive break rates to 667,8 and 720,2 m/s accordingly. Taking into account the safety factor of 1.4 we will get the maximum cutting speed of 484.2 and 543.0 m/s respectively.

Table 2. Grinding wheel body calculation results from different materials.

№	Grinding wheel body material	Permissible tensile stress, $[\sigma]$, MPa	Density, ρ , kg/m ³	Maximum allowable linear break rate, V_r , m/s			Maximum permissible operating speed with safety factor in mind, V_r , m/s		
				a	b	c	a	b	c
1.	AlCu4Mg1	460	2770	576,6	340,0	411,6	242,8		
2.	C45	600	7800	392,2	231,4	280,2	165,3		
3.	13Kh11N2 VMF-Sh	950	7800	493,5	291,2	352,5	208,0		
4.	25KhGSA	1080	7850	524,6	309,4	374,7	221,0		
5.	VT3-1	1180	4500	724,2	379,3	517,3	270,9		
6.	VT22	1280	4620	746,0	440,1	532,9	314,3		
7.	VT15	1500	4500	816,5	481,7	583,2	344,0		
8.	30KhGSN 2A	1620	7770	645,7	380,9	461,2	272,1		
9.	03H18K9 M5T	1920	8050	688,5	406,2	491,8	290,1		

Titanium alloy VT3-1 is of higher quality in comparison with other materials and existing structures due to its lower density and high tensile strength. However, due to its density and correspondingly the final weight of the grinding wheel, the use of this material is limited by its vibration resistance, i.e. the design does not have sufficient vibration resistance. Therefore, the material 30KhGSN2A capable of providing the required cutting speeds at vibration disturbances was used [16-17].

5 Experimental results and discussion. Grinding wheel load and stress analysis

Calculation and distribution of stresses in a grinding wheel was made by a method of finite elements with application of calculation and analytical program ANSYS. The work presents the calculations of strength, static strength, elastic and elastic plastic calculations. The author considers two variants of a arrangement of machining elements: horizontally and at an angle of 45 degrees and offers designs (figure 5 and 6). The arbor and spindle are also calculated.

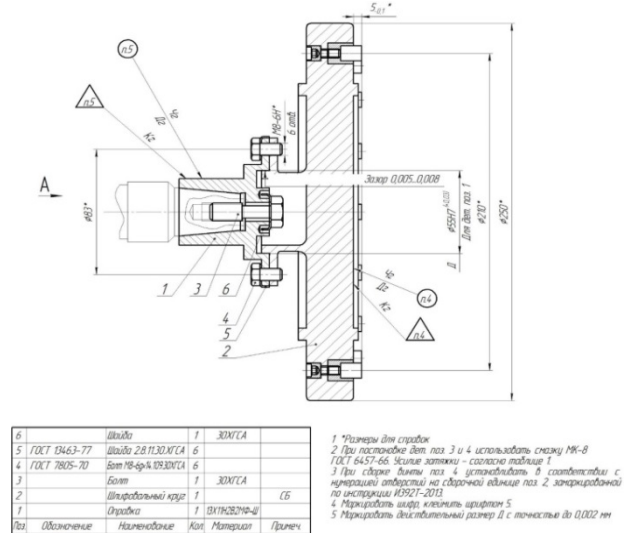


Fig. 5. Grinding wheel for ultra-fast grinding with horizontal machining units

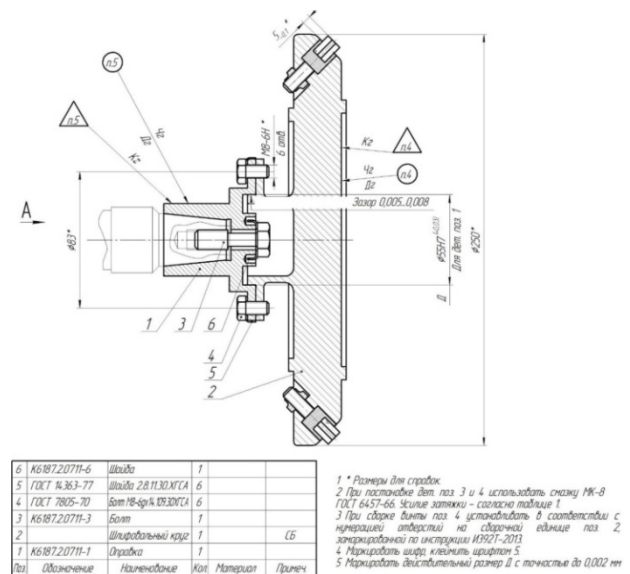


Fig. 6. Grinding wheel for ultra-fast grinding with 45 degree grinding angles

The developed high-speed grinding and grinding wheel has the following main parameters:

- 1) maximum circle diameter up to 250 mm;
- 2) maximum width up to 40 mm;
- 3) maximum working speed up to 400 m/s;
- 4) number of machining elements - 16 pieces;
- 5) two arrangement options for the machining elements.

The grinding wheel consists of the body and the machining elements. Body material - 13Kh11N2V2MF-Sh ($\sigma_{0,2} = 950$ MPa). Properties of the material: $E = 196200$ MPa (20000 kgf/mm²) – modulus of elasticity; $\mu = 0,3$ – Poisson's ratio; $\sigma_v = 1100$ MPa – tensile strength; $\sigma_{0,2} = 950$ MPa – yield strength; $\delta = 1,5\%$ – percentage elongation; $H = 1360$ MPa – hardening module; $\rho = 7,8$ g/sm³ – density.

The weight calculation of the grinding heads is shown in Table 3. With horizontal arrangement $M = 21,718$ g, with 45-degree machining position $M = 29,663$ g.

Table 3. Grinding head weight calculation.

Location head	Details	Material	Density ρ , g/s ³ m ³	Dimensions			Volume V , mm ³	Mass M , g	
				D , mm	d , mm	L , mm			
Horizontal	Body	Abrasive	4,15	10	3	13	929,13	3,856	
	Bucket	C45	7,8	14	10	8	603,19	4,705	
			7,8	14	6	5,9	741,42	5,783	
			7,8	9	0	2,1	133,6	1,042	
			7,8	9	5	2,1	94,5	0,737	
	Screw	13Kh11 N2V2M F-Sh 1	7,8	6	0	8	226,19	1,764	
			7,8	4,5	0	4	63,617	0,496	
			7,8	10	0	9	706,86	5,513	
			7,8	8,4	0	3	-166,3	-1,297	
			7,8	6	0	4	-113,1	-0,882	
							21,718		
At an angle 45 degrees	Body	Abrasive	4,15	10	3	13	929,13	3,856	
	Bucket	C45	7,8	14	10	8	603,19	4,705	
			7,8	14	0	6	923,63	7,204	
			7,8	9	0	2	127,23	0,992	
			7,8	9	5	2	90	0,702	
			7,8	8	0	20	1005,3	7,841	
	Nut		7,8	14	8	4,5	466,53	3,639	
			7,8	9,5	8	4,5	92,775	0,724	
								29,663	

Centrifugal force of grinding heads with horizontal arrangement $C = 30156 \text{ N}$ (3074 kgf), with an angle of 45 degrees $C = 32108 \text{ N}$ (3273 kgf).

Housing with horizontal grinding heads

The volume solid model of the grinding wheel body is built. A sector (1/6 part) is cut out of the body. This sector is taken as a calculation model. The cyclo-symmetric model is fixed along the axis of rotation and in the circumferential direction[18-20].

Elements in the form of a tetrahedron are used to generate a finite element grid. The sector is divided into $NEL = 1796237$ finite elements and contains $KN = 316998$ nodes. Calculation of the stress-strain state (SSS) of the wheel is made from the action of centrifugal forces occurring in the body, and from the centrifugal forces of grinding heads $C = 30156 \text{ N}$ (3074 kgf). Operating speed $n = 34725 \text{ min}^{-1}$ ($\omega = 3636 \text{ rad/s}$). Figures 7-9 show the results of the case SSS under working conditions. The greatest stresses are in the grinding head holes and are local in nature. Equivalent voltages in them $\sigma_e^{max} = 942 \text{ MPa}$. Equivalent plastic deformation in the holes $\epsilon_p = 0,035\%$. Voltages in the astragal molding of the carrier in fabric 875 MPa. Voltages in the hub 803 MPa.

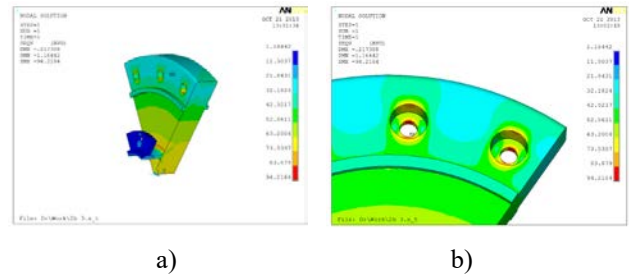


Fig. 7. Equivalent stresses in sector (a) and grinding head holes (b).

Radial movements:

flange holes (83 mm diameter) $UR = 0.0163 \text{ mm}$;
 holes for grinding heads (105 mm diameter) $UR = 0.184 \text{ mm}$.

Axial movements holes for grinding heads on the abrasive side (105 mm diameter) $UZ = 0.065 \text{ mm}$. The housing is evenly stretched out in radial direction and narrowed in axial direction.

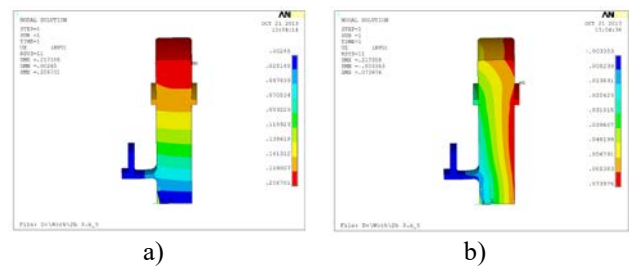


Fig. 8. Radial movements (a) and axial movements (b).

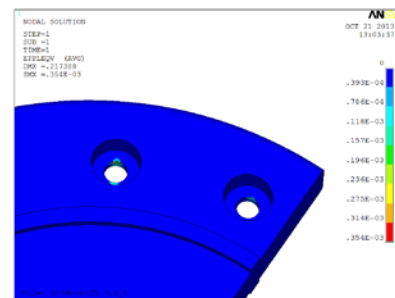


Fig. 9. Equivalent plastic deformation.

When calculated according to the two-dimensional scheme of the stress state with stress averaging on the thickness of the disk, the safety margin $K_m = 1.651$ in the center of the disk. Allowance for destructive rotational speed $K_v = 1.425$. Stocks are sufficient.

Enclosure with angled grinding heads

The volume solid model of the grinding wheel body is built. A sector (1/16 part) is cut out of the body. This sector is taken as a calculation model. The cyclo-symmetric model is fixed along the axis of rotation and in the circumferential direction.

Elements in the form of a tetrahedron are used to generate a finite element grid. The sector is divided into $NEL = 898532$ finite elements and contains $KN = 160671$ node. Calculation of the stress-strain state (SSS) of the wheel is made from the action of centrifugal forces arising in the body and from the centrifugal forces of grinding heads $C = 32108 \text{ N}$ (3273 kgf). Operating

speed $n = 30558 \text{ min}^{-1}$ ($\omega = 3200 \text{ rad/s}$). Figures 10-12 show the SSS on the hull under working conditions

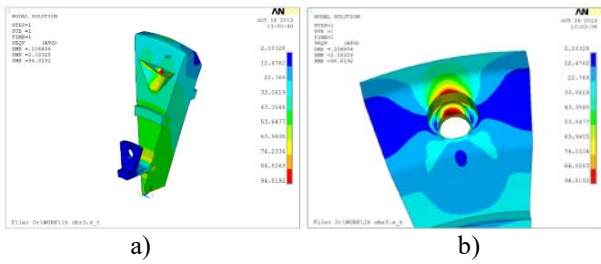


Fig. 10. Equivalent tensions in sector (a) and into the grinding head opening (b).

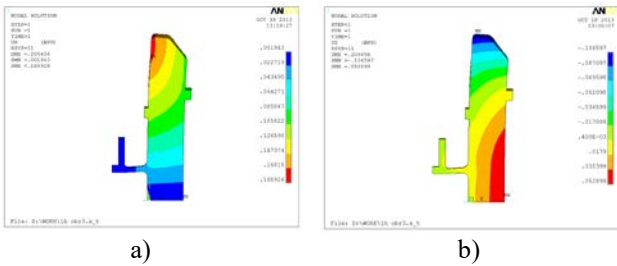


Fig. 11. Radial movements (a) and axial movements (b).

The greatest stresses are in the grinding head holes and are local in nature. Equivalent voltages in them $\sigma_{ekq}^{max} = 948 \text{ MPa}$. Equivalent plastic deformation in the holes $\varepsilon_p = 0,3\%$. Voltages in the astragal molding of the carrier in fabric 722 MPa. Voltages in the hub 604 MPa.

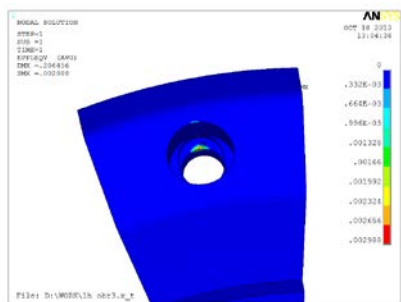


Fig. 12. Equivalent plastic deformation

Radial movements:

flange bores (83 mm diameter) $U_R = 0,0137 \text{ mm}$;
 grinding head bores on the abrasive side (105 mm diameter) $U_R = 0,127 \text{ mm}$.

Axial movements:

grinding head holes on the abrasive side (105 mm diameter) $U_Z = 0,07 \text{ mm}$.

The body in the central part is evenly stretched out radially and narrowed axially. The periphery of the casing bends to the abrasive side. When calculated according to the two-dimensional scheme of the stress state with stress averaging on the thickness of the disk, the safety margin $K_m = 2.132$ in the center of the disk. Inventory at destructive speed $K_v = 1.619$.

Calculating mandrel and spindle

In order to assess the failure to open the joint between the spindle and mandrel, calculations of these elements from the action of centrifugal forces were

made. Figures 13 and 14 show the equivalent stresses and radial movements. At the points of contact between the spindle and mandrel, the mandrel displacement is $3 \mu\text{m}$, while the spindle displacement is $0.5 \mu\text{m}$. This results in a conicity of $1:5$ to the axial displacement of the mandrel by $\delta = (3 - 0.5) \cdot 5 \cdot 2 = 25 \mu\text{m}$.

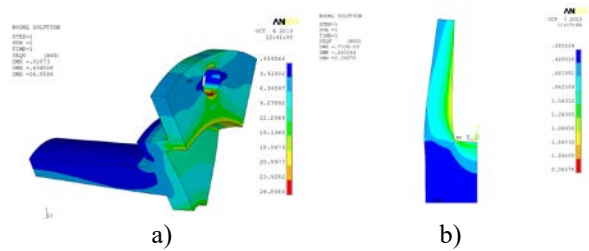


Fig. 13. Equivalent stresses in mandrel (a) and spindle (b).

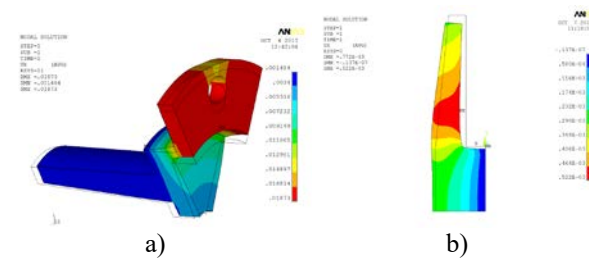


Fig. 14. Radial movements in mandrel (a) and spindle (b).

This movement causes the tightening to be loosened. For this reason, a special flow screw has been designed to compensate for axial movement.

Radial displacement of flange bores (83 mm diameter) $U_R = 0.017 \text{ mm}$, almost identical to the movements of the housing flange.

6 Conclusion

This work leads us to the following conclusions:

1. The strength of high-speed grinding wheels has been calculated. Two variants of arrangement of machining elements are considered: horizontally and at an angle of 45 degrees. The horizontal version of the grinding heads is preferable. The casing deforms uniformly without bending. Manufacturing this casing is less time-consuming.
2. The mandrel and spindle are calculated. According to calculations, a special screw with a flow was designed to compensate the axial movement of the mandrel relative to the spindle.
3. Radial movements in the area of the flange holes (83 mm in diameter) at the housing and mandrel are nearly the same.

Acknowledgments

The work was carried out with the financial support of the Grant Council of the President of the Russian Federation for state support of young Russian scientists and for state support of leading scientific schools of the Russian Federation, grant number MD-345.2020.8.

References

1. M.M. Paley, *Grinding and grinding technology of the cutting tool* / M.M. Paley, L.G. Dibner, M.D. Flyd (M.: Mashinostroenie, 1988)
2. Pat. 101666 Russian Federation, MPK B 24 D 7/06. Grinding wheel for high-speed machining / D.S. Rechenko, K.V. Averkov, A.Yu. Popov; applicant and owner of OmGTU - № 2010139548/02; de clared. 24. 09.2010; o p. 27.01.2011, Bulletin No. 3. – 2 c.: silt.
3. Pat. 1 46505 Russian Federation, IPC B 24D 3/32. Grinding tool / D.S. Rechenko, B.P. Kudryashov, A.Yu. Popov; applicant and owner of OmGTU - № 2014123264/02; de clared. 06. 06.2014; o p. 10.10.2014, Bulletin No. 28. – 1 c.: silt.
4. Pat. 2440229 Russian Federation, IPC B 24B 1/00, B24B 9/ 16, B 28D 5/ 02. Method of superhard materials processing / D.S. Rechenko, A.Yu. Popov. 08.02.2010; op. 20.01.2012, Bulletin No. 2. – 1 c.
5. Pat. 2547980 Russian Federation, IPC B 24B 3/36. Method of sharpening the metal-cutting tool blade with a grinding wheel / D.S. Rechenko, A.Yu. Popov; applicant and owner of OmGTU - № 2013142129/02; de clared. 13. 09.2013; op. 10.04.2015, Bulletin No. 10. – 1 c.
6. Pat. 55665 Russian Federation, MPK B 24D 17/00. Grinding wheel for diamond and abrasive machining / D.S. Rechenko, Yu.R. Nurtdinov, A.Yu. Popov; applicant and owner of OmGTU - № 2006111080/22; de clared. 05.04.2006; o p. c it. 27.08.2006, Bulletin No. 24. - 2 p.: silt.
7. D.S. Rechenko, *Improvement of quality of the high-speed sharpening of the carbide tools by the diamond circles with the interrupted surface*: (Dissertation ... Cand. of Sciences, Tomsk, 2009)
8. V.A. Rybitskiy, Synthetic diamonds., **3**, 32–35 (1978)
9. L.N. Filimonov, *High-speed grinding* / L.N. Filimonov. - L.N (Filimonov: Mashinostroenie, Leningr. departing, 1979)
10. L.N. Filimonov, *Grinding wheel resistance* / L.N. Filimonov. - L.N (Filimonov: Mashinostroenie, 1973)
11. D.S. Rechenko, A.G. Kol'tsov, Russian Engineering Research, **32**(2), 179 – 181 (2012)
12. D.S. Rechenko, A.Y. Popov, K.V. Averkov, V.A. Sergeev, Russian Engineering Research, **32**(5-6), 511 – 512 (2012)
13. L. Tian, Y. Fu, J. Xu, H. Li, W. Ding, International Journal of Machine Tools & Manufacture, **89**, 192–201 (2015)
14. C. Wang, Q. Fang, J. Chen, Y. Liu, T. Jin, International Journal of Advanced Manufacturing Technology, **83**, 937–948 (2016)
15. L. Yang, Y. Fu, J. Xu, Y. Liu, Materials and Design, **88**, 827–836 (2015)
16. Z. Zhao, Z. Fu, J. Xu, Z. Zhang, The International Journal of Advanced Manufacturing Technology, **87**, 3545–3555 (2016)
17. Y. Zhu, W. Lu, Y. Sun, D. Zuo, The International Journal of Advanced Manufacturing Technology, **89**, 1269–1277 (2017)
18. S.N. Grigoriev, V.A. Grechishnikov, M.A. Volosova, X. Jiang, P.M. Pivkin, In IOP Conference Series: Materials Science and Engineering, **971**(2), 022065 (2020) doi: 10.1088/1757-899X/971/2/022065
19. S.N. Grigoriev, P.M. Pivkin, V.A. Grechishnikov, Y.E. Petukhov, M.A. Volosova, A.B. Nadykto, Emerging Imaging and Sensing Technologies for Security and Defence V; and Advanced Manufacturing Technologies for Micro-and Nanosystems in Security and Defence II, **11540**, 115401E (2020) <https://doi.org/10.1117/12.2574389>
20. S.N. Grigoriev, M.A. Volosova, A. A. Okunkova, S.V. Fedorov, K. Hamdy, P.A. Podrabinnik, ... , A.N. Porvatov, J. Manuf. Mater. Process., **4**(3), 96 (2020) <https://doi.org/10.3390/jmmp4030096>